SEMARAK ILMU PUBLISHING

Journal of Advanced Research in Fluid Mechanics and Thermal Sciences

Journal homepage:
https://semarakilmu.com.my/journals/index.php/fluid_mechanics_thermal_sciences/index
ISSN: 2289-7879

Performance Study of NePCM-nanofluid based PVT System

Fahim Rahim Sheikh[1,*], Suresh Pandurang Deshmukh[1], Purushottam Ardhapurkar[2], Md Modassir Hussain[3], Pankaj Wankhede[4], Vikramsinha Korpale[1], Tushar Sathe[4]

[1] Department of General Engineering, Institute of Chemical Technology, Mumbai, India
[2] Department of Mechanical Engineering, Mauli Group of Institution's College of Engineering and Technology, Shegaon, India
[3] Department of Mechanical Engineering, SVKM's Institute of Technology, Dhule, India
[4] Department of Mechanical Engineering, S. B. Jain Institute of Technology Management and Research, Nagpur, India

ARTICLE INFO

Article history:
Received 10 April 2024
Received in revised form 8 July 2024
Accepted 17 July 2024
Available online 15 August 2024

Keywords:
Hybrid PVT collectors; nanofluid; nano-PCM; paraffin wax

ABSTRACT

Photovoltaic thermal (PVT) systems integrated with Nanoparticle Enhanced Phase Change Materials Nanofluid (NePCM-nanofluid) are widely used in solar thermal systems for thermal energy storage, and they significantly improve energy efficiency. Solar thermal systems are particularly viable in the region of high-temperature and variable climatic conditions. It is crucial to understand the NePCM-nanofluid PVT systems' performance in this regard to adapt the technology to the hot regional conditions. Four solar systems—PV, PVT, PVT-PCM, and PVT-NePCM-nanofluid—were tested in Shegaon, Vidarbha, India, under real-time conditions. Integration of PVT-NePCM-nanofluid reduced PV cell temperature by 25.7°C during peak radiation. Comparative analysis revealed electrical efficiencies of 12.40% to 14.50% and thermal efficiencies ranging from 40% to 70%. The experimental analysis has been carried out at varied flow rate of nanofluid and optimal system performance was observed at a 7 LPM flow rate.

1. Introduction

The amount of solar energy that reaches Earth's surface is 6000 times more than what is used globally, much of it going wasted by people. In hot climatic regions like in India, this enormous potential is significant. 300 days a year, eight hours of sunshine are received in many parts of the nation, and daily solar energy averages between 6-7 kWh/m^2 [1]. Based on this data, the country has an abundance of solar resources that it may use to further sustainable development and meet its energy needs. As per Ministry of New and Renewable Energy (MNRE), Maharashtra, ranks third in solar energy potential in India [2]. Given the immense solar potential in India, particularly in regions like Maharashtra, where solar energy is abundant, it is crucial to investigate technology such as PVT systems to improve energy capture. As we explore ways to enhance the use of solar energy, it is essential to consider the importance of effectively controlling temperatures in photovoltaic (PV) systems [3]. Ensuring optimal photovoltaic efficiency, minimizing thermal degradation, and

* *Corresponding author.*
E-mail address: fahimsheikh786@gmail.com

https://doi.org/10.37934/arfmts.120.1.1334

maintaining constant and reliable energy output are essential in changing environmental circumstances. The PVT system's efficiency mainly depends on the surface temperature and is inversely proportional [4]. To regulate the temperature effectively, it is necessary to have a cooling system that can eliminate the solar heat responsible for PVT heating [5].

PVT cooling systems can be categorized into integrated technologies and developing technologies. The available technologies for cooling are passive cooling, active cooling, and a hybrid of active-passive cooling systems [6,7]. Active cooling systems necessitate the utilization of operate without an external power source. Developing technologies encompass liquid immersion cooling, phase change materials cooling, colorless and transparent silicon shielding, Peltier-based thermo-electric cooling, and microporous evaporation foils [8]. To obtain optimal efficiency of the solar cells, it is necessary to implement a cooling system alongside the heating of the solar panels. Nanofluids, active cooling fluids, have demonstrated a potential ability to transmit heat due to their high thermal conductivity. Nanofluids consist of nanoparticles, such as carbides, metals, semiconductors, and single and multi-walled nanotubes, ranging in size from 1 to 100 nm. These nanoparticles are mixed with base fluids, such as water and ethylene [9,10]. The cooling efficiency of nanofluids is contingent upon the optimal combination of nanoparticles and base fluids.

Many research studies focus on the Phase Change Material (PCM) based cooling fluids to improve the efficiency of PVT systems, with higher heat capacitance, thus absorbing more heat from the cell. Paraffin wax is a common PCM material. It is inexpensive, non-toxic, environmentally friendly, and has a wide operating temperature range for PVT applications [11-13]. Al-Imam *et al.,* [14] investigated the thermal and electrical efficiency of a compound parabolic concentrator (CPC) PVT system using PCM in an outdoor experiment. They found overall PVT efficiencies on sunny and semi-cloudy days of around 55-63% and 46%-55%, respectively. Browne *et al.,* [15] also found that PCM PVT systems increase overall efficiency. Hasan *et al.,* [16] investigated the role of PCM in the building-integrated PV (BIPV) system. The study reveals that among five different types of PCMs studied, the most significant decrease in cell temperature was around 18 OC. Kazanci *et al.,* [17] investigated the use of PCM in a PVT system for heating and cooling a house. It was been found that the PVT efficiency was approximately 42.8% and the standalone PV efficiency was 13.59%. Hasan *et al.,* [18] studied the overall energy for a solid-liquid PCM-based PV system in two different climates. According to the findings, Ireland and Pakistan achieved average efficiencies of 14.6% and 20.3%, respectively. For an HVAC application, Fiorentini *et al.,* [19] investigated an air-based PVT system with a PCM storage unit incorporated in a reverse cycle heat pump, generating 9% electrical efficiency and 45% thermal efficiency. However, the improvement in electrical efficiency is not enough to increase accountability. So, researchers in this area tried incorporating the nanofluids with the PVT systems.

Karunamurthy *et al.,* [20] improved the thermal conductivity of paraffin PCM by incorporating CuO nanoparticles, thus improving the heat transfer rate of the thermal energy storage system. Khanjari *et al.,* [21] explored using nanofluid as an alternative to water for cooling a PVT system. Use of a nanofluid instead of water for a better thermal conductor was found essential for this system. To describe the motion of nanofluid, alumina-water, and pure water, CFD analysis was found as helpful tool. The author discovered that the base fluid's heat transfer efficiency improved with the increased quantity of nanoparticles. Nanofluids made of alumina and water have a heat transfer coefficient 12.1% higher than plain water and 43.1% higher than Ag-water. Rejeb *et al.,* [22] examined the potential effects of nanofluids as heat transfer agents in a PVT system using a computer model based on FORTRAN. The results were compared with an early empirical model. The intended PVT system was tested in three locations—Lyon, France; Mashhad, Iran; and Monastir, Tunisia—to observe the impact of weather on the findings. According to the research, water was utilized as the base fluid, and found more effective than ethylene glycol. It has been observed that thermal conductivity increased with nanoparticle suspension concentrations ranging from 0% to 4%. According to the data, the electrical and thermal performance was highest in the coldest semiarid climate, which is located in Monastir, Tunisia. Minea [23] studied the thermophysical features of three oxide-based nanoparticles to determine better material among Al2O3, TiO2, and SiO2when used in water; performing numerical studies. Scientists found that introducing nanoparticles changed the thermophysical properties of every tested material and increased its thermal conductivity by 12% or more. The nanofluid's thermal conductivity and Reynolds number improved with an increase in nanoparticle concentration, raising the convection heat transfer coefficient.

Sardarabadi *et al.,* [24] investigated the efficacy of a PVT-phase change material system chilled with ZnO-water NF. This experiment used paraffin wax instead of phase change material (PCM). The electrical exergy efficiency was 23% higher and the performance was 13% better than that of traditional PV modules when using the proposed phase change material/NF hybrid system. Hosseinzadeh *et al.,* [25] experimented with a PVT-phase change material system chilled by ZnO-water NF to determine its efficiency. The proposed PVT-phase change material cooled with NF outperformed the control system thermodynamically. Compared to conventional photovoltaic (PV) and water-based PVT-phase change material cooling systems, the proposed system improved energy efficiency by 65.71% and exergetic efficiency by 13.61%. Hassan *et al.,* [26] examined how graphene water could handle heat and control temperature in a PVT-phase change material system. The experimental parameters used for the studies were ϕv=0.05%, 0.1%, 0.15% and Q=20, 30, and 40 LPM. The Al box and Cu tube transfer the molten phase change material (RT35HC) to the winding flow channel networks on the module's lower surface. The graphene-water-cooled PVT system achieved the highest η_{EE}, η_{TE}, and η_{ov} at Q = 40 LPM and ϕv = 0.1%, as shown by the findings. The percentages were 14.0%, 45.8%, and 60.3% respectively.

Based on a thorough examination of existing literature, it is observed that, researchers have mainly focused on improving the efficiency of PVT panels by using Phase Change Materials (PCM) and nanofluids. Nevertheless, few researchers have investigated the simultaneous use of both approaches synergistically. Significantly, with the Indian context, there has been a lack of studies examining this integrated strategy. In the current article, a novel attempt to design a new PVT system that can effectively combine nano-enhanced PCM and SiC-based nanofluids to boost the performance of a traditional PVT system is presented. The fully developed system underwent extensive testing using multiple combinations of fluids, and the performance of the PVT system was systematically compared across these various configurations. It includes a NePCM-nanofluid-based PVT system with PV, PVT, and PVT-PCM systems.

2. Methodology

The present study employed an active cooling system based on forced water circulation to cool the PV module with an external power source. The various components necessary for the system were designed and fabricated following a thorough literature review.

2.1 Experimental Set-up

The experimental setup for the PVT system is constructed using various components as shown in Table 1. The experimental investigations are conducted at the Mauli Group of Institutions College of Engineering and Technology in Shegaon, Maharashtra, India, with coordinates 20.7930° N, 76.6910° E. The orientation of the experimental setup was kept southward, inclined at a slope of 19°. The outdoor conditions during the experimentation period included an average temperature of approximately 24 °C, a wind speed of 10 km/h, and humidity at 95%. The PVT system's design comprises a PV panel connected to a tank filled with a phase change material (PCM).

Table 1
Various components with specification used in the experimental setup

Sr. No	Components	Parameters	Units	Quantity
1	PV Panel		Watt	4
2	Water tank			2
3	Pump		HP	2
4	Flow control valve	-	-	3
5	Rotameter	Flow rate	Lit/min	3
6	Nano fluid tank			1
7	Heat exchanger			1
8	K-type thermocouples	Temperature	^{O}C	8
9	PT-100 (RTD)	Temperature	^{O}C	6
10	Data logger	Temperature	^{O}C	1
11	MS602-Pyranometer		KW/Hrs	1
12	Atmospheric temperature sensor	Temperature	^{O}C	
13	Multimeter	Voltage and current	V and A	4

In the present research work paraffin wax is used as the PCM, mixed with nano-SiC particles to optimize charging, and discharging processes. To improve heat transfer and overall performance, a separate closed-cycle fluid flow system carrying nanofluid is integrated into the tank to transfer heat to an external heat exchanger. The effectiveness of this PVT design is estimated using four experimental setups: standalone PV system, PVT system attached to a water-filled container with water as the working fluid, PVT system connected to a PCM-filled container with water as the working fluid, and PVT system attached to a nanoparticles-dispersed PCM-filled container with nanofluid as the working fluid. Data from all PVT systems and PV systems are collected simultaneously. Figure 1 illustrates the schematic diagram and experimental setup, including a supporting pole for PV panels, water pumps, a nanofluid container, a hot water storage tank, a laptop, and a data acquisition system.

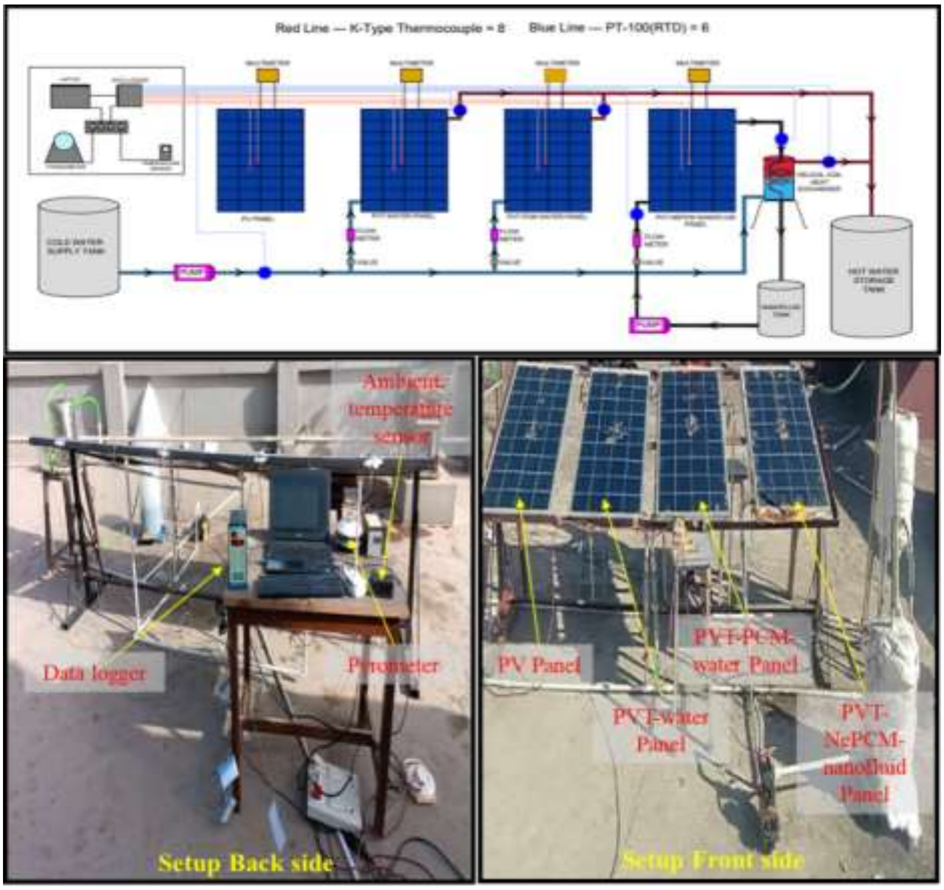

Fig. 1. Experimental setup

A 50 mm thick layer of glass wool is applied around the PCM container to prevent heat leakage to the atmosphere. Figure 2(a) displays the designed and fabricated absorber used in the study, emphasizing the critical role of the collector's area in determining thermal efficiency. The chosen circular tube absorber minimizes the collector's area while maintaining optimal thermal contact with the PV module. Figure 2(b) illustrates a schematic with fabricated PCM and NePCM aluminium containers. The container includes two pipes at the top, one serving as an inlet for the PCM and the other for releasing hot vapor. A layer of silicon oil is applied between the PV panel and the aluminium container to eliminate air gaps and enhance the collector's thermal capacitance, as shown in Figure 2(c).

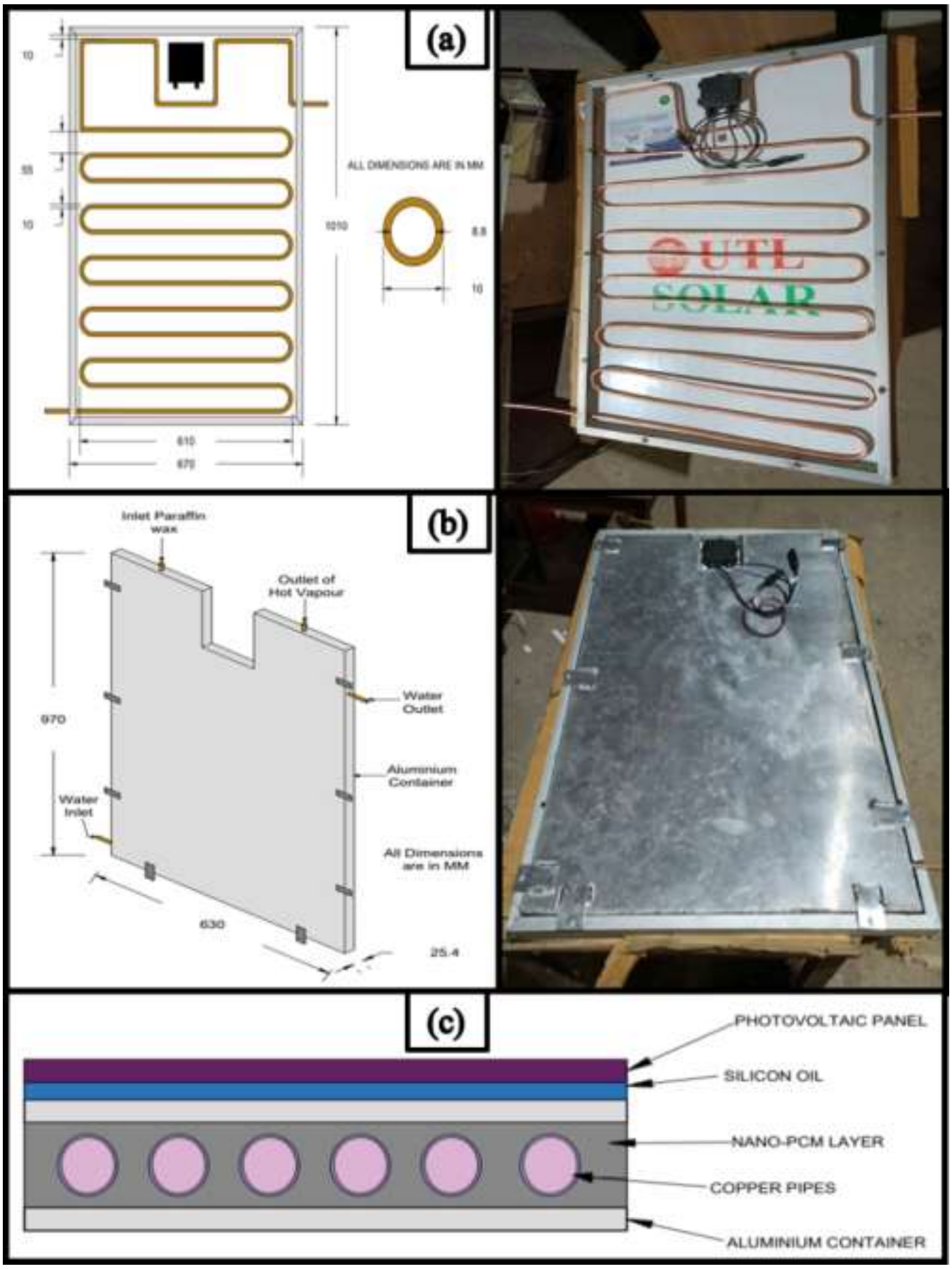

Fig. 2. (a) Designed and fabricated absorber, (b) PCM and NePCM aluminium containers, (c) Cross section of the assembled PVT system

Table 2 shows the dimensional parameters of the helically coiled tube heat exchanger. The copper-made circular tubes allow efficient heat transfer to the water in the heat exchanger. The heat exchanger used is indirect, comprising an internal heat exchanger. A horizontal stainless-steel cylinder of 600 mm in length and 250 mm in diameter is insulated with 50mm thick glass wool. Figure 3 shows the designed and fabricated heat exchanger.

Table 2
Dimensional parameters of the helically coiled tube

Helically coiled tube (Copper)	Dimensions	Shell (Stainless steel)	Dimensions
Tube's internal diameter	18.5 mm	Shell's external diameter	250 mm
Tube's external diameter	20 mm	Shell's internal diameter	240 mm
Tube's effective length	5000 mm	Shell's Length	600 mm
Pitch of the coil	40 mm		
Number of turns in the coil	13		

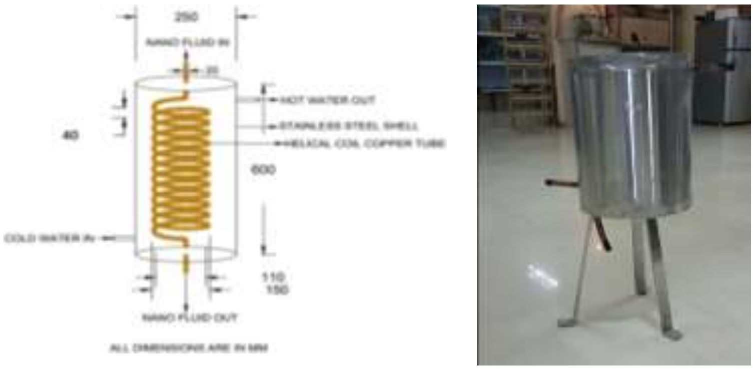

Fig. 3. Helical coil tube heat exchanger

2.2 Preparation of Nanofluids

The silicon carbide (SiC) nanoparticles with properties detailed in Table 3 were procured from US Research Nanomaterials, Inc., USA. Initially, these nanoparticles were preheated at 200°C for approximately one hour to eliminate unwanted moisture. The nanofluid was then formed by suspending SiC nanoparticles by weight percentage in deionized water. During the first 30 minutes, the mixture underwent agitation in an ultrasonic bath shaker. Subsequently, an ultrasonic probe sonicator was employed for about 6 hours to disperse any remaining nanoparticle agglomeration. This was followed by 60 minutes of magnetic needle stirring at 600 rpm, using a magnetic stirrer setup to achieve a homogeneous and stable suspension.

Table 3
Specification of the used nanomaterial

Item	Silicon carbide Nano powder specifications
Manufacturer	US Research Nanomaterials, Inc., USA
Appearance	Grayish white powder
Purity	99+%
PH value	3–7 at 20 °C
Grain size nm	45–65 nm
Crystal and Type	Cubic
Bulk density g/cm3	3.22
Lose on drying %≤	0.21
Melting point °C	2730
Thermal conductivity (W/m·K)	370–490

This method was employed to generate nanofluids at various concentrations (1, 2, 3, and 4%); the FESEM image of silicon carbide nanoparticles is presented in Figure 4(a), revealing nanoparticles ranging in size from 40 to 60 nm. Nanofluid density was determined using the Liquid Density Tester. To measure nanofluid viscosity for variable volume concentrations at different temperatures, a Rheometer interfaced with a personal computer for data collection and storage was utilized. The thermal conductivity of the nanofluids was measured using a KD2-pro thermal conductivity meter. All relevant density, viscosity, and thermal conductivity tests were conducted thrice to ensure repeatability, and the average value was considered to minimize uncertainty stemming from random measurement errors.

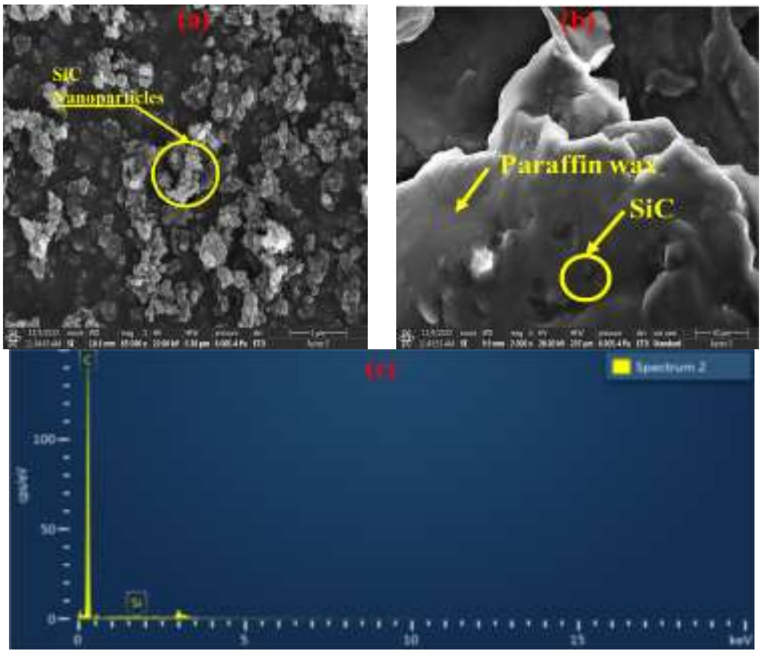

Fig. 4. Scanning electron microscopy and EDX (a) SEM of SiC nanoparticles, (b) SEM of SiC-Paraffin wax mixture, (c) EDX for Paraffin/nano-SiC

2.3 Preparation of Nano-PCM

The samples were prepared by blending paraffin with SiC nanopowder. The nanoparticle mass fraction values (wt.%) dispersed in the paraffin wax were 0%, 0.1%, 0.5%, 1%, 2%, 3%, and 4%. The mixing process was carried out using an Ultrasonic Shaker, which provided heating (800W) and thorough shaking of the samples for 60 minutes (30 kHz). This process ensured no sedimentation, optimal dispersion, and homogeneous and stable suspension formation. Two stages of testing were conducted on these samples. The first stage involved a visual test to observe color changes and assess homogeneity in all prepared paraffin wax-nano-SiC samples. Color changes and homogeneity serve as the initial evidence of the complete amalgamation of nanoparticles in wax. The second stage consisted of thermo-physical properties testing to measure fluidity, viscosity, and thermal conductivity, confirming the enhancements paraffin received. The properties of the tested paraffin wax are detailed in Table 4. Once a specific mass fraction is determined from the tests, it is employed for relatively large-scale production of the PCM container.

Table 4
Characteristics of the Paraffin Wax

Material properties	Range
Melting point temperature (°C)	46 and 68 °C
Density (kg/m^3)	900 kg/m3
Viscosity	16-18
Thermal conductivity (W/m °C)	0.20

Figure 4(b) presents a FESEM image of silicon carbide nanoparticles with paraffin, demonstrating its presence in the 40 to 60 nm range. The SiC-paraffin sample underwent further analysis through Electron Dispersion X-ray (EDX) imaging and Electron Dispersion Spectroscopy (EDS) (Figure 4(c)). EDX and EDS are effective techniques for determining the morphological composition of substances smaller than one cubic micron. This equipment is attached to a scanning electron microscope (SEM) to collect elemental information from the sample under examination. X-ray diffraction (XRD) was also employed to image the SiC-paraffin samples. These various images validate the state and properties of the mix, providing a comprehensive understanding of the impact of using SiC nanoparticles in paraffin.

3. Results

Experiments were conducted on the roof of the Mechanical Engineering Department, Mauli Group of Institutions College of Engineering and Technology in Shegaon, Maharashtra, India. The experiments were conducted on six sunny days in February and March from 8.30 am to 5.30 pm for all cases PV, PVT, PVT-PCM, and PVT-NePCM-nanofluid in parallel, and results are compared for analysis. The effect of six different flow rates from 5, 6, 7, 8, 9 and 10 LPM were investigated.

3.1 Thermo-physical Properties of Nanofluid and NePCM

Thermophysical properties of base fluid changed with addition of nanoparticles. These changes affect heat transfer property of the nanofluid. Variable thermal conductivity standards of a nanofluid depend a lot on its preparation technique. Tests focused on measuring the nanofluids' density, viscosity, and thermal conductivity to ascertain its effect on heat movement were performed.

The density measurements on nanofluid were marked from 25°C to 60°C, and variations were observed at 0.994, 1.002, 1.014, and 1.014 g/ml for fractions of 1, 2, 3, and 4% nanoparticles. Up to the addition of 3% nanoparticle SiC, the growth rate was minimal at best. Density followed the same pattern as nanofluid viscosity. For 1, 2, 3, and 4 SiC nanoparticle fractions, the increases in viscosity close to pure water were 0.93388, 2.3956, 3.3606, and 4.7139 (mPa.s.), respectively. The highest viscosity rise was seen at 25 C after adding a 2 wt% concentration of SiC nanoparticles; after that, the rate of increase became less effective. Improving thermal conductivities over base fluids is the primary goal of nanofluid research. About the nano-SiC fractions, the thermal conductivities enhanced over deionized water were 0.51, 0.76, 0.68, and 0.82 W/m°C for nano-SiC fractions of 1, 2, 3, and 4%, respectively. When making nanofluids, there are many things to consider, like choosing suitable materials, efficiently making nanomaterials, and using the proper solvent. Every three months, the thermal conductivity of the SiC-nanofluid being used for studies was checked. After six months, the drop in thermal conductivity did not go over 0.70 W/m°C. This shows that mixing water with SiC nanoparticles without particles getting agglomerate together was a good idea.

Paraffin wax's thermal conductivity and capacity are more important than changes in density and viscosity since it is not a flowing material in the system like the nanofluid. At 25 °C, the density showed variations of (0.005, 0.01, 0.02, 0.024, 0.028) for the (0.1, 0.5, 1, 2, 3 %) respectively, added SiC mass fractions. As the wax's viscosity increased by (0.05, 0.20, 0.25, 0.32, and 0.40 %) according to the addition of (0.1, 0.5, 1, 2, 3% of nano-SiC), the influence of the addition of nano-SiC on the viscosity became more accurate. Adding nano-SiC to the PCM boosted its thermal conductivity; the nanoparticle mass concentration was 0.1% of the wax weight for 14 kg. Adding different concentrations of nano-SiC to wax improved its thermal conductivity, but the effect was small and did not justify the higher cost of the system. For this reason, adding 0.1% nano-SiC mass fraction to the paraffin wax was decided upon. Since it is tiny and has no adverse effect on the system's cost, this ratio improved the wax's thermal conductivity.

3.2 Analysis of Ambient Condition

Figure 5 displays the temporal changes in solar radiation and ambient temperature over six days. Solar radiation's intensity progressively increases from 12:15 pm to 1:15 pm and then declines. The solar radiation intensity peaked at 850 W/m² to 922 W/m².

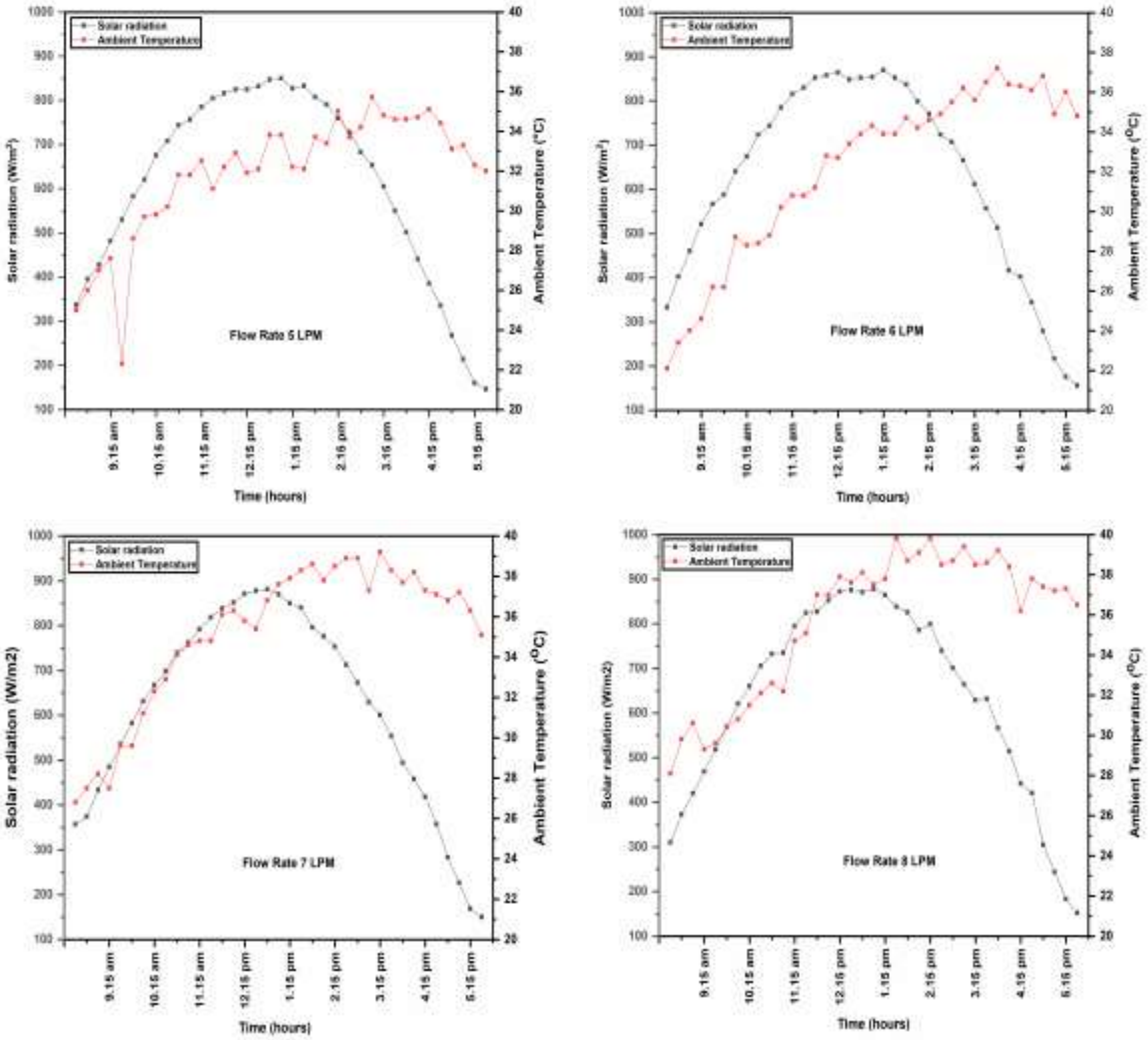

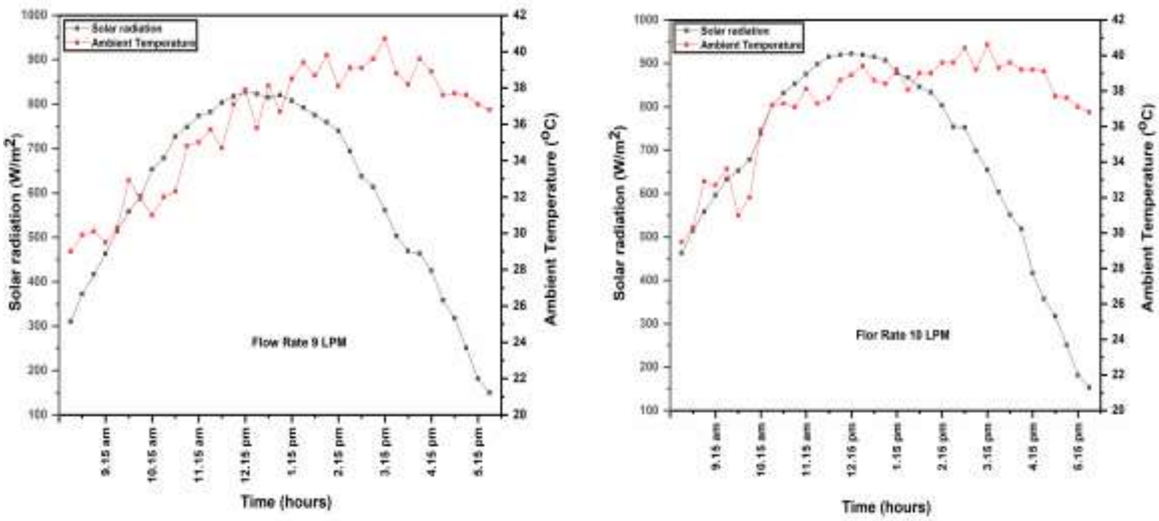

Fig. 5. Variation in solar radiation and ambient temperature at different flow rates

The ambient temperature had an upward trajectory until 3:15 pm, after which it began to decrease. The highest recorded temperature during these studies ranged from 35°C to 41°C.

3.3 Analysis of Electrical Power

The electrical power is calculated by measuring the voltage and current with the help of a voltmeter and ammeter installed separately on each PV module. Figure 6(a) shows the variation in electrical power for the entire module PV, PVT, PVT-PCM, and PVT-NePCM-nanofluid, along with solar radiation and time. It also shows the effect of variation in the electrical power with different flow rates.

It is observed that the electrical power is higher in the case of PVT-NePCM-nanofluid compared to PV, PVT, and PVT-PCM for all the flow rate cases. Figure 6(b) shows the electrical higher power in the PVT-NePCM-nanofluid case than in all flow rates. A maximum of 7 LPM flow rate produced higher power with maximum solar radiation intensity on that day. Figure 6(a) depicts the trends in electrical power obtained over time for all tested instances at 5, 6, 7, 8, 9, and 10 LPM working fluid flow rates, respectively. Due to increased solar radiation, electrical power grew with time until midday but then declined. Among all other situations, 7 LPM performed the best at all flow rates.

At 5 LPM, the maximum power achieved was 87.47 W, 89.81 W, 92.15 W, and 101 W for PV, PVT, and PVT-PCM cases, respectively. PV electrical power for PVT was increased by 3.24%, PVT-PCM electrical power was increased by 8.09%, and PVT-NePCM-nanofluid electrical power was increased by 17% at a 7 LPM flow rate concerning stand-alone PV system.

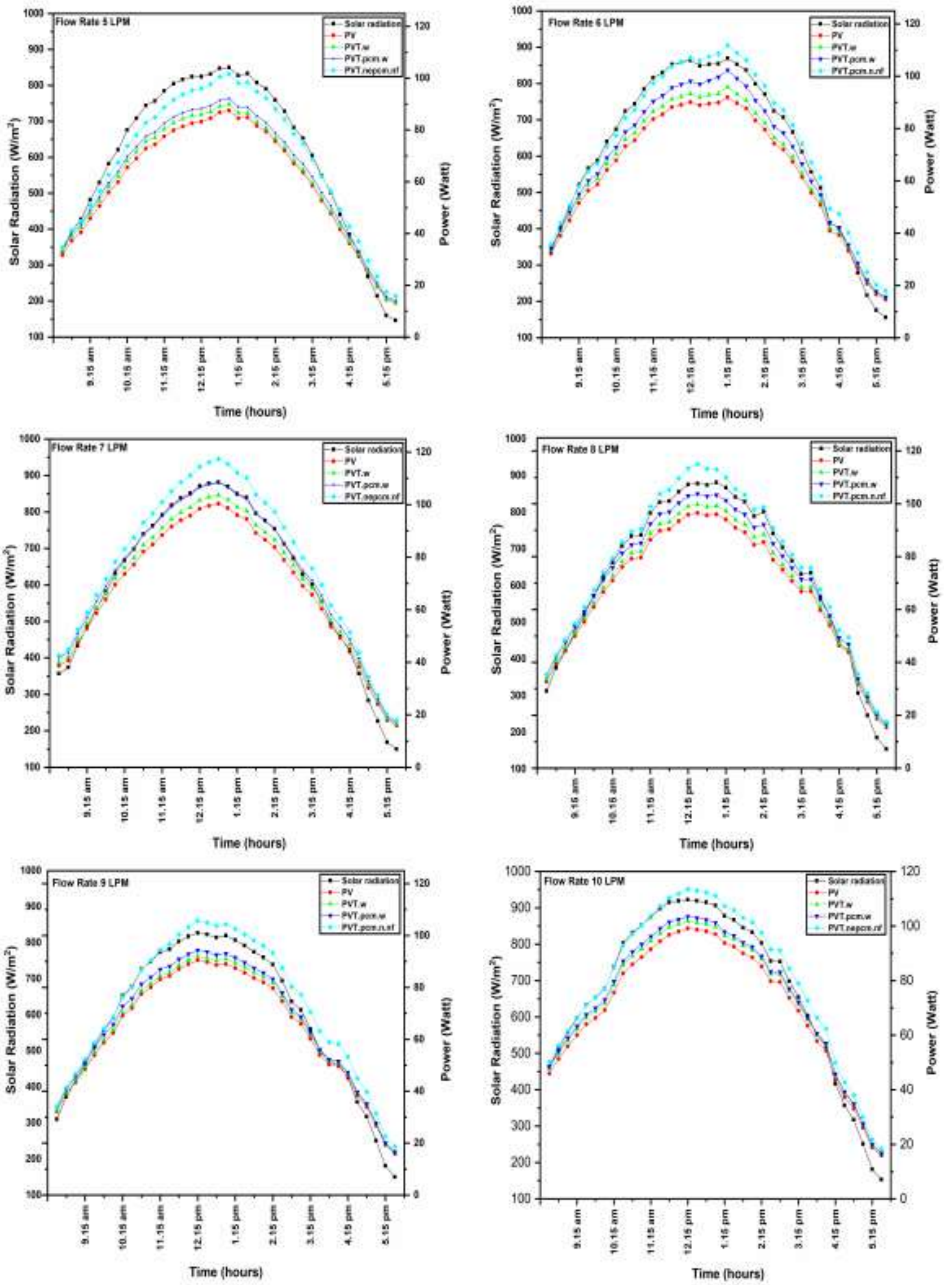
Flow Rate 5 LPM
Flow Rate 6 LPM
Flow Rate 7 LPM
Flow Rate 8 LPM
Flow Rate 9 LPM
Flow Rate 10 LPM
Solar radiation
PV
PVT.w
PVT.pcm.w
PVT.nepcm.nf
PVT.pcm.n.nf
Solar Radiation (W/m²)
Power (Watt)
Time (hours)
9.15 am
10.15 am
11.15 am
12.15 pm
1.15 pm
2.15 pm
3.15 pm
4.15 pm
5.15 pm

(a)

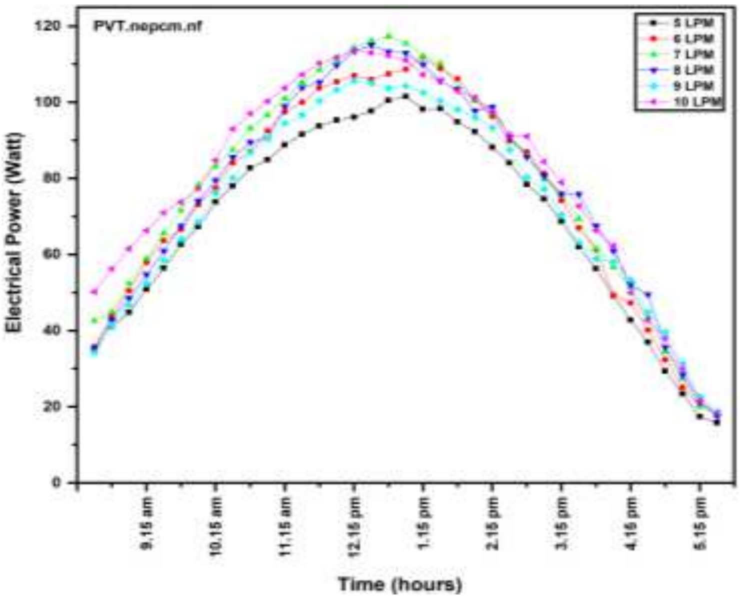

(b)

Fig. 6. (a) Electrical power vs Time vs solar radiation at different flow rates for all the considered cases, (b) Effect of flow rate on electrical Power of PVT-NePCM-nanofluid of system

3.4 Variable Systems Temperature and Water Outlet Temperature

Figure 7 depicts the front PV temperature profiles throughout the day with a working fluid flow rate of 5, 6, 7, 8, 9 & 10 LPM. Compared to the naturally-cooled PV panel, all PV panels showed reduced cell temperature. It also offers the water outlet temperature of PVT, PVT-PCM, and PVT-NePCM-nanofluid at different flow rates. At nearly 1 pm, the maximum PV temperature for cases PV, PVT, PVT-PCM, and PVT-NePCM-nanofluid was 66.8°C, 48.8°C, 46.3°C, and 43.1°C, respectively. PVT-NePCM-nanofluid achieved the most significant temperature reduction compared to PV, PVT, and PVT-PCM. Similarly, the maximum decrease in PV temperature was observed for PVT-NePCM-nanofluid at a working fluid flow rate of 6 LPM. At 6 LPM, peak PV temperatures were measured around 1.15 pm to be 66.9°C, 47.9°C, 45.1°C, and 41.4°Cfor cases PV, PVT, PVT-PCM, and PVT-NePCM-nanofluid, respectively.

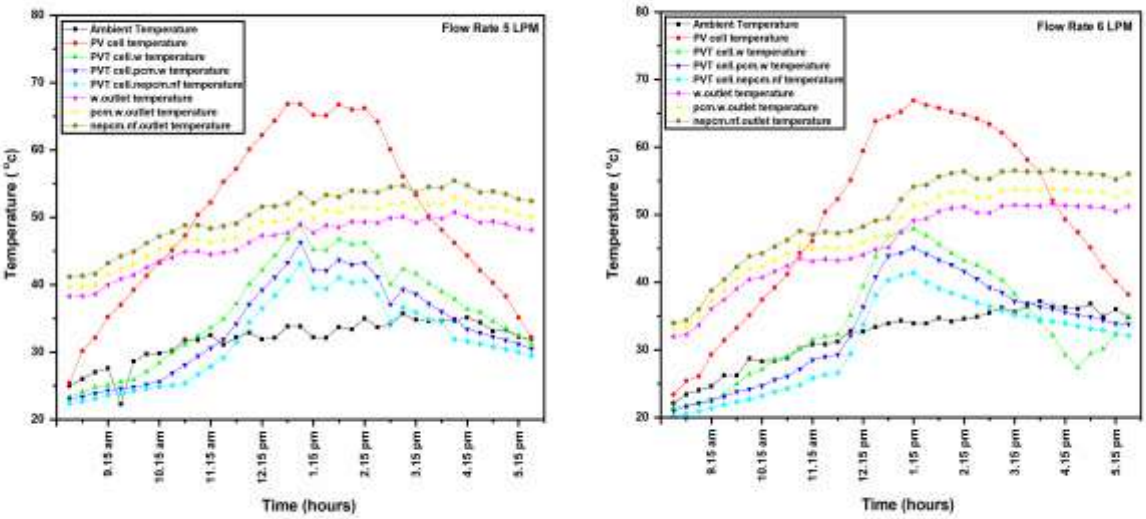

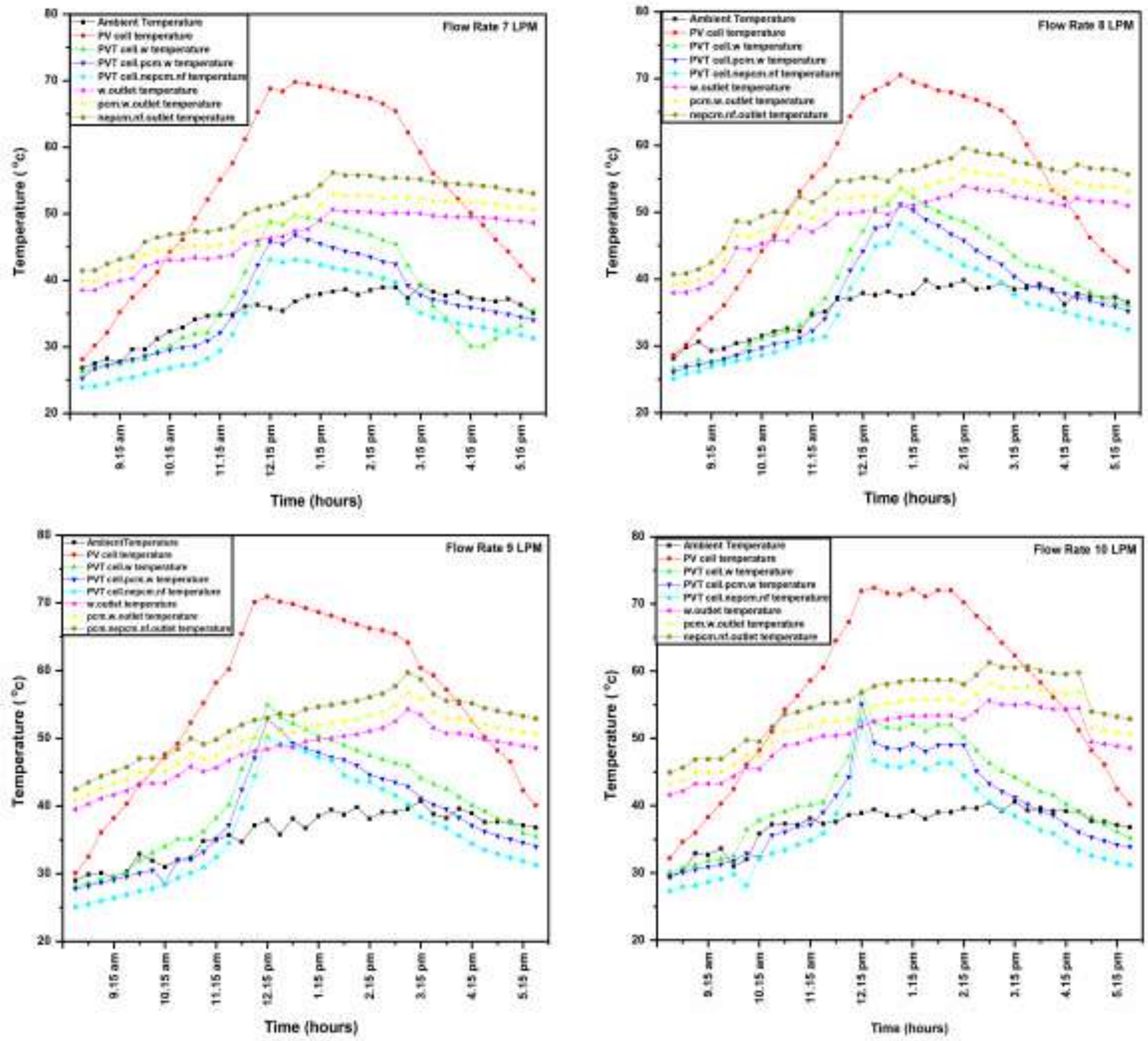

Fig. 7. Variable systems temperature distribution with time

A similar pattern was observed for flow rates of 7. At 7 LPM, peak PV temperatures for cases PV, PVT, PVT-PCM, and PVT-NePCM-nanofluid were 69.8°C, 49.8°C, 46.8°C, and 43.1°C, respectively. Peak PV temperatures were 70.5°C, 53.5°C, 51.2°C, and 48.2°C for cases PV, PVT, PVT-PCM, and PVT-NePCM-nanofluid, respectively, at 8 LPM. Peak PV temperatures for 9 LPM were found to be 70.9°C, 54.9°C, 52.9°C, and 50.1°C for cases PV, PVT, PVT-PCM, and PVT-NePCM-nanofluid, respectively. Similarly, the peak PV temperatures for 10 LPM were 71.9°C, 56.9°C, 55.1°C, and 52.6°C for cases PV, PVT, PVT-PCM, and PVT-NePCM-nanofluid, respectively. As a result, at all flow rates, the PVT system integrated with PVT-NePCM-nanofluid demonstrated the most significant reduction in PV temperature. The most extraordinary drop in surface temperature occurred at a flow rate of 7 LPM. The drop in temperature at this flow rate is due to the flow of a large amount of fluid through the channel in the optimum time required for maximum heat absorption from the system, thus allowing the PV surface to cool. The fluid's outlet temperature rises steadily over time. The heat is transferred from the PVT cell to water at different flow rates. At a mass flow rate of 7 LPM, the maximum water and nanofluid outlet temperature is obtained. As compared to water, nanofluids exchange more heat from PVT cells. At higher flow rates, the outlet temperature is lower.

3.5 Analysis of Electrical Efficiency

Figure 8(a) shows the variation in electrical efficiency for all the modules of PV, PVT, PVT-PCM, and PVT-NePCM-nanofluid, along with solar radiation and time. It also offers different working fluid flow rates at 5, 6, 7, 8, 9, and 10 LPM.

For PV, PVT, PVT-PCM, and PVT-NePCM-nanofluid cases, the average PV efficiency at 5 LPM was 11.2%, 11.5%, 11.8%, and 13%, respectively. Like electrical power, electrical efficiency showed an increasing trend with the coolant flow rate. The electrical efficiency obtained at 6LPM was 11.5%, 12%, and 14%, respectively. Similarly, at 7 LPM, this was found to be 12.4%, 12.8%, 13.4%, and 14.5%. The electrical efficiency obtained at 8LPM was 12%, 12.4%, 12.9%, and 14.3%. The electrical efficiency obtained at 9LPM was 11.9%, 12.1%, 12.4%, and 13.9%. Similarly, at 10 LPM, the electrical efficiency obtained was 11.7%, 12%, 12.2%, and 13.4%, respectively. The application of NePCM and nanofluid increased the electrical efficiency of PV systems. This combination of NePCM and Nanofluid assisted in lowering the temperature of the PV surface, which increased electrical efficiency. The NePCM-nanofluid module achieved the highest electrical efficiency because the surface temperature of the PVT system was the lowest when compared to other PVT, PVT-PCM and conventional PV. The higher thermal conductivity of nanoparticles enables more heat removal from the system in less time than water. The electrical efficiency for flow rates of 7 LPM was greater than that of other flow rates, as shown in Figure 8(b).

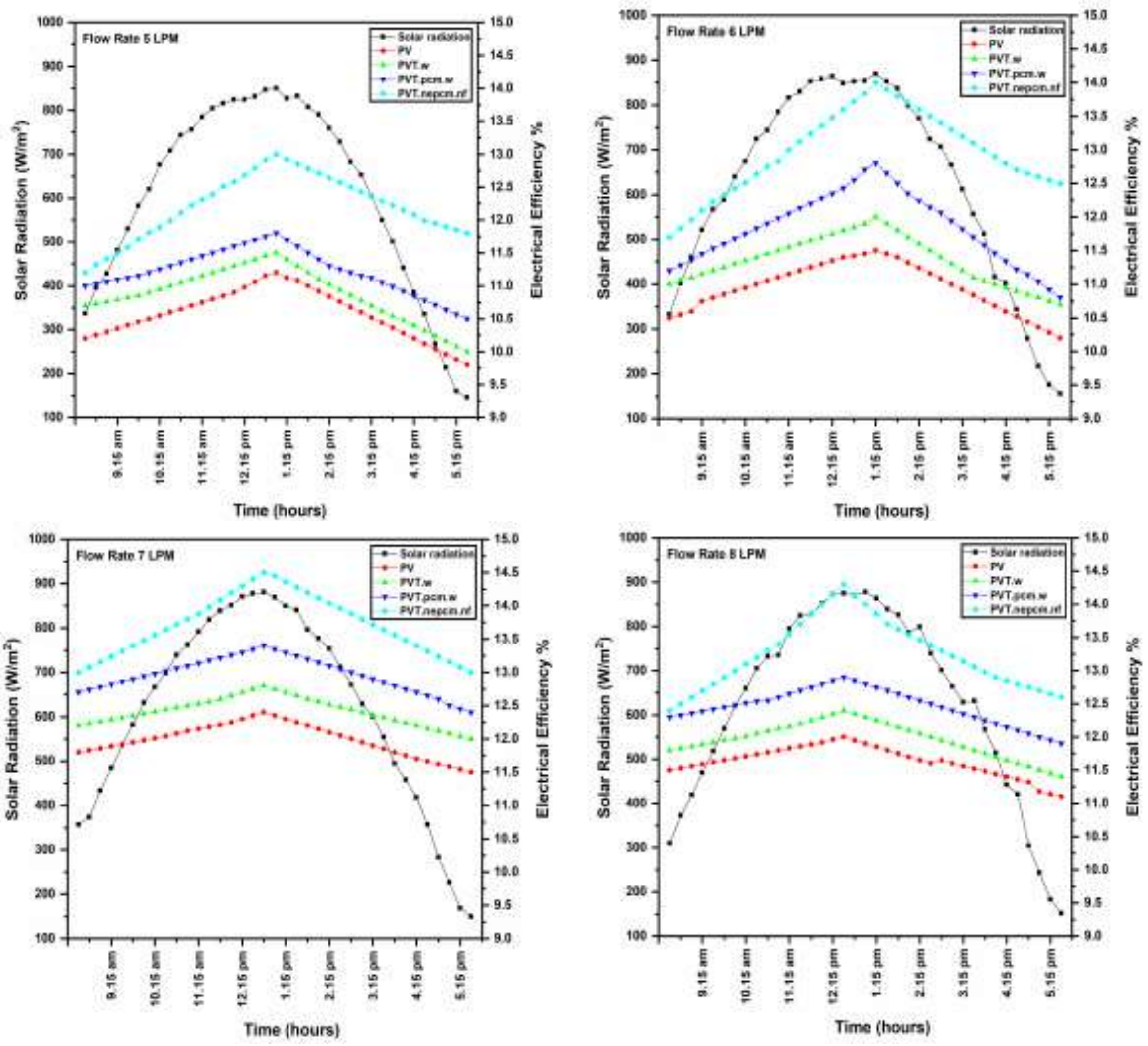

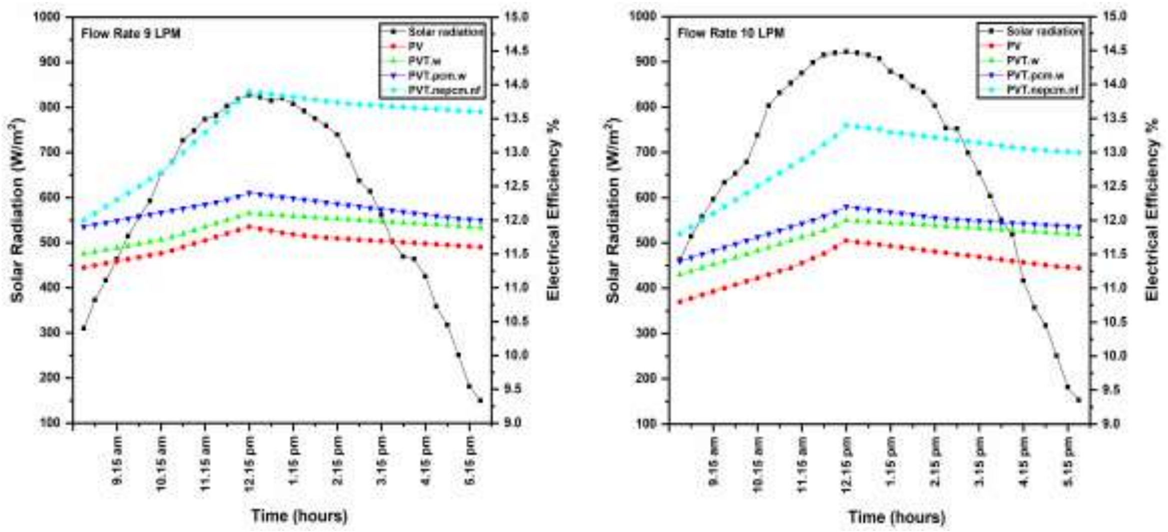

(a)

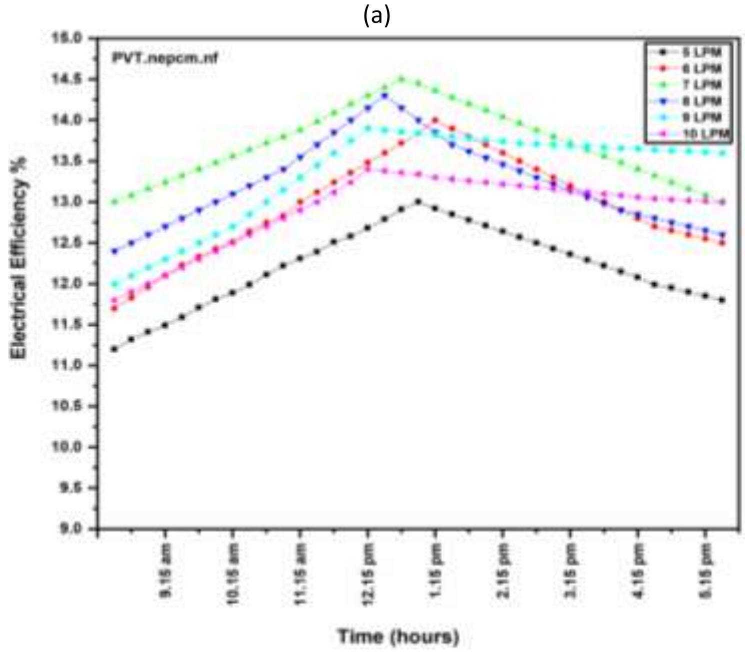

(b)

Fig. 8. (a) Electrical efficiency vs time vs Solar radiation for all cases, (b) Effect of flow rate on Electrical Efficiency of NePCM of system

3.6 Analysis of Thermal Efficiency

Figure 9(a) shows the variation in thermal efficiency for modules PVT, PVT-PCM, and PVT-NePCM-nanofluid along with time at different flow rates. It was also observed that thermal efficiency is higher in the case of PVT-NePCM-nanofluid than PVT & PVT-PCM for all the flow rate cases, as shown in Figure 9(b). Thermal efficiency at 5 LPM was determined to be 36%, 39%, and 40% for cases PVT, PVT-PCM, and PVT-NePCM-nanofluid, respectively, as shown in Figure 9(a). It also offers similar trends for flow rates of 6, 7, 8, 9, and 10 LPM. At 6 LPM, thermal efficiency was 36%, 40%, and 50%, respectively. The thermal efficiency of the PVT system was increased by increasing the flow rate. Still, at 7 LPM, the thermal efficiency is higher because, at higher flow rates, the temperature difference between the inlet and outlet of the PVT system was increased due to the high heat absorption of the system's nanofluid. Thermal efficiency was observed at 7 LPM for cases PVT, PVT-PCM, and PVT-NePCM-nanofluid to be 40%, 50%, and 70%, respectively.

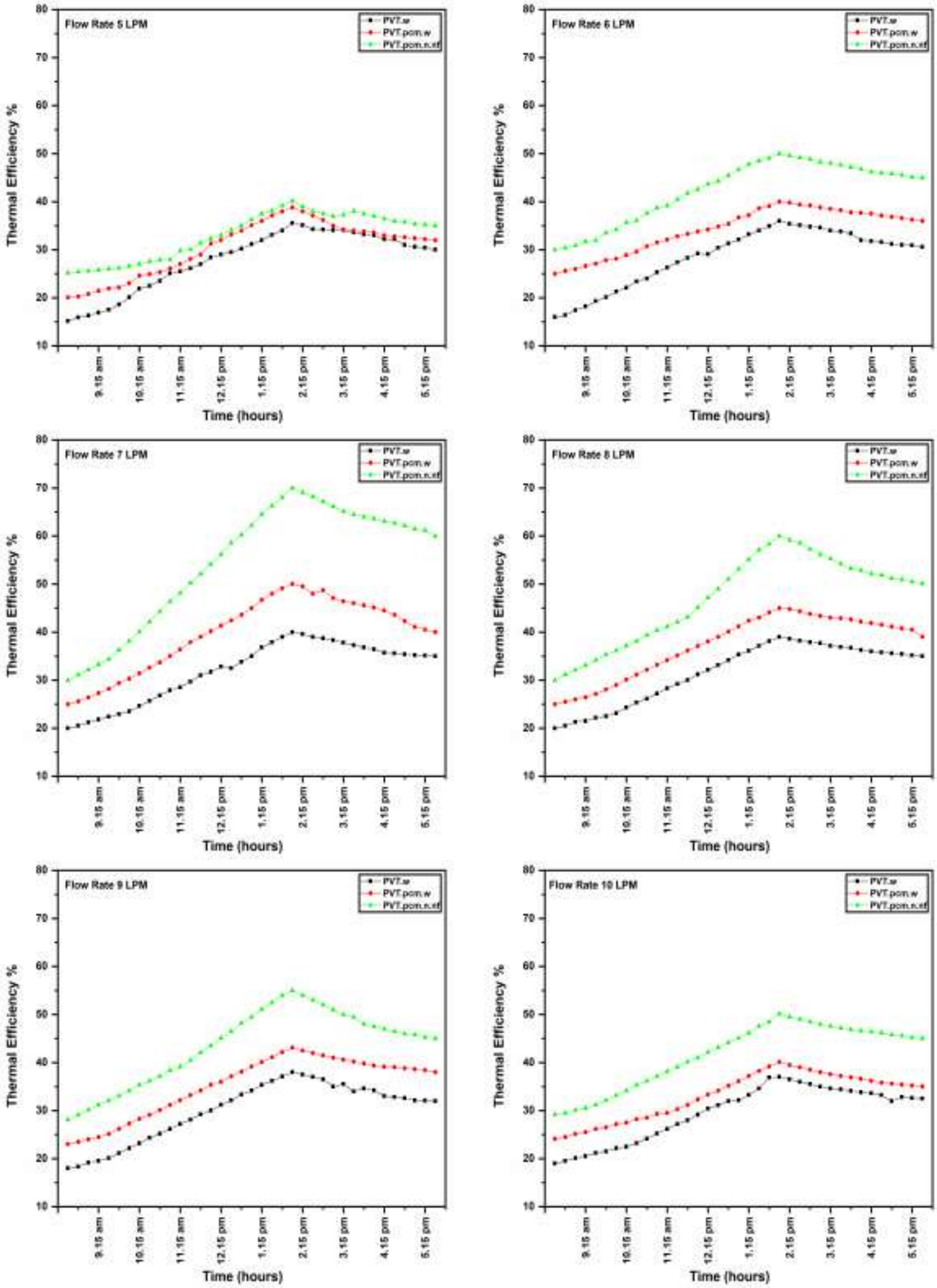
Flow Rate 5 LPM
Flow Rate 6 LPM
Flow Rate 7 LPM
Flow Rate 8 LPM
Flow Rate 9 LPM
Flow Rate 10 LPM
PVT.w
PVT.pcm.w
PVT.pcm.n.nf
Thermal Efficiency %
Time (hours)
9.15 am
10.15 am
11.15 am
12.15 pm
1.15 pm
2.15 pm
3.15 pm
4.15 pm
5.15 pm

(a)

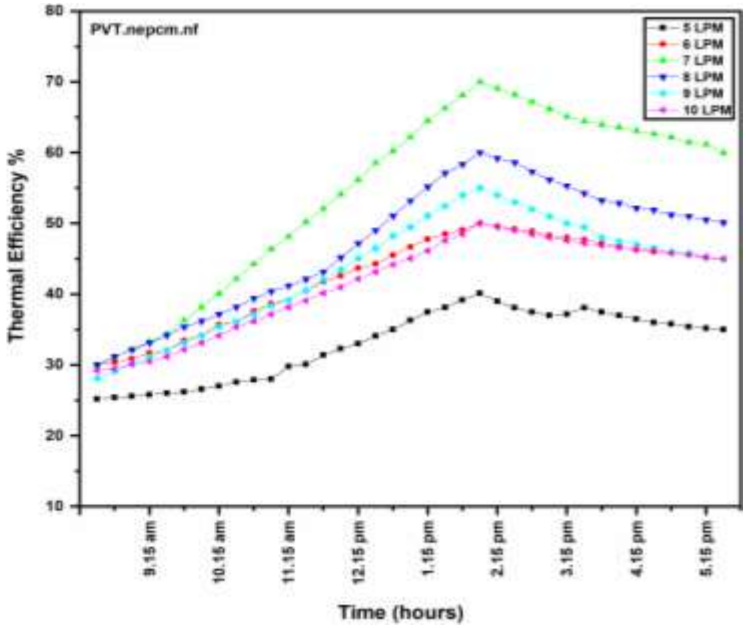

(b)

Fig. 9. (a) Thermal efficiency vs time at different flow rates, (b) effect of flow rate on Thermal Efficiency of PVT-NePCM-nanofluid system

At 8 LPM, thermal efficiency was 39%, 45%, and 60%, respectively. At 9 LPM, thermal efficiency was 38%, 43%, and 55%, respectively. At 10 LPM, thermal efficiency was 37%, 40%, and 50%, respectively. Compared to water, the thermal efficiency of the PVT-NePCM-nanofluid was increased by 20% at a flow rate of 7 LPM.

3.7 Analysis of Overall Efficiency

Figure 10(a) shows the overall efficiency calculated by the combination of electrical & thermal efficiency of cases PVT, PVT-PCM, and PVT-NePCM-nanofluid at different flow rates of 5 to 10 LPM. It is observed that the PVT-NePCM-nanofluid overall efficiency is higher as compared to PVT and PVT-PCM. At 5 LPM, the overall efficiency of PVT, PVT-PCM, and PVT-NePCM-nanofluid cases is 46.66%, 50.20%, and 52.86%, respectively. Overall efficiency at 5 LPM and 10 LPM follows the same pattern as at 5 LPM. At 6 LPM, the efficiency increases in the following order: 47.70%, 52.35%, and 63.70%. Similarly, at 7 LPM, overall efficiency is 52.56%, 63.15%, and 84.12%. Similarly, at 8 LPM, overall efficiency is 51.1%, 57.6%, and 73.54%. Similarly, at 9 LPM, overall efficiency is 50.03%, 55.35%, and 68.76%.

At 10 LPM, overall efficiency is 48.93%, 52.18%, and 63.35%. The effect of flow rate on overall efficiency at PVT-NePCM-nanofluid is shown in Figure 10(b). The 7 LPM flow rate overall efficiency is higher than other flow rates.

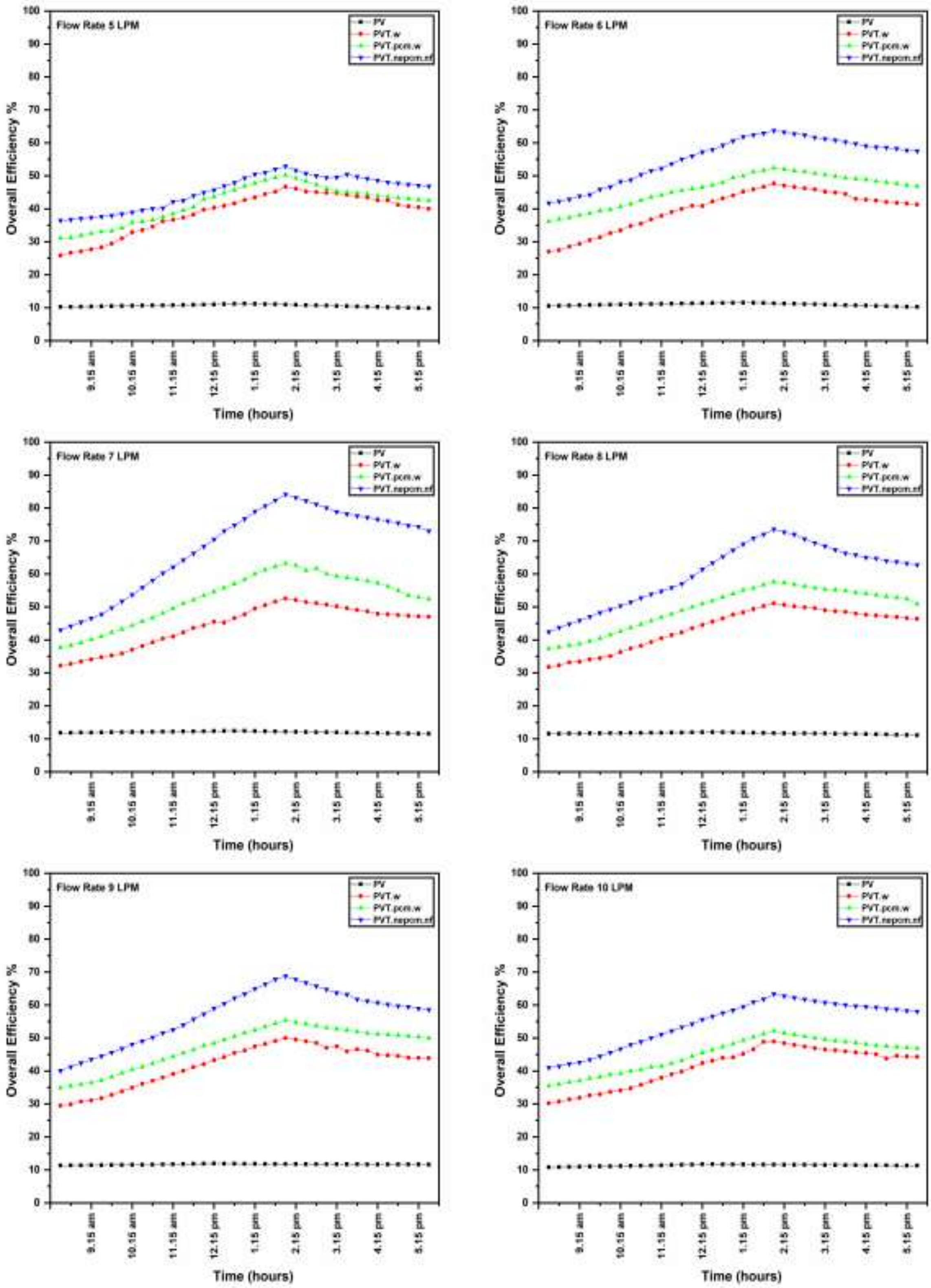
Flow Rate 5 LPM
Flow Rate 6 LPM
Flow Rate 7 LPM
Flow Rate 8 LPM
Flow Rate 9 LPM
Flow Rate 10 LPM
PV
PVT.w
PVT.pcm.w
PVT.nepcm.nf
Overall Efficiency %
Time (hours)
9.15 am
10.15 am
11.15 am
12.15 pm
1.15 pm
2.15 pm
3.15 pm
4.15 pm
5.15 pm

(a)

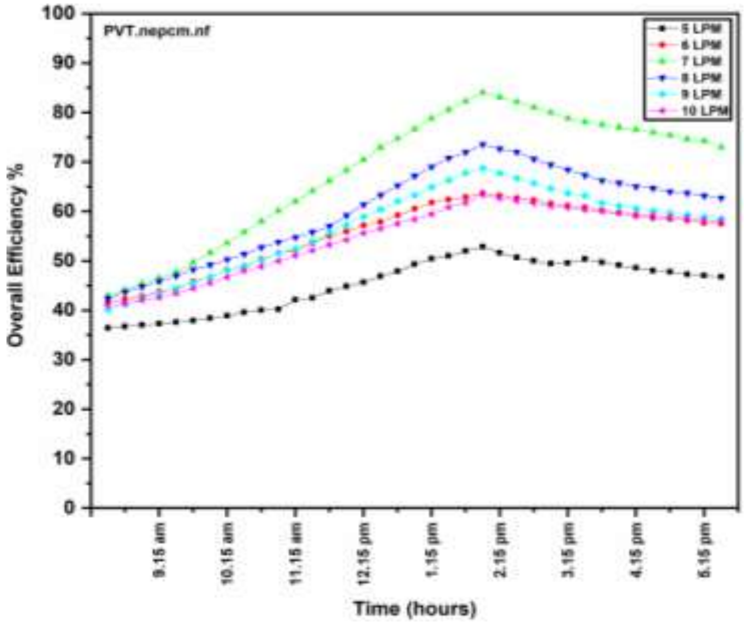

(b)

Fig. 10. (a) Overall efficiency vs time, (b) Effect of flow rate on Overall Efficiency of PVT-NePCM-nanofluid system

4. Conclusions

The performance of PVT system is evaluated in this research work by comparing four different systems as: the standalone PV system, the PVT system with water cooling, the PVT system with PCM and water cooling, and the PVT system with NePCM/nano-SiC cooling. Furthermore, the impact of different flow rates of the working fluid on the performance of the PVT system is investigated. The key findings from the present research work are as follows

i. The overall efficiency of all the considered systems is maximum for the fluid flow rate of 7 LPM. Thus the 7 LPM can be considered as an optimum flow rate of circulating fluid for mentioned ambient conditions and location. Thus, it can be concluded that the performance of PVT system largely depends on the flow rate of circulating fluid.
ii. The PVT system, which utilizes NePCM-nanofluid and operates at a flow rate of 7 LPM, demonstrates a significant reduction of 62% in the surface temperature of the PV panel compared to other PVT systems.
iii. It is observed that the electrical efficiency is improved by 2.50 % in the PVT with NePCM-nanofluid system compared to other PVT systems for optimum fluid flow rate.
iv. The thermal efficiency of PVT system with water, PVT with water and PCM, and PVT with NePCM-nanofluid systems are 40 %, 50%, and 70% respectively.
v. The overall efficiency of the PVT with NePCM-nanofluid system is calculated at varied flow rate of fluid as: 5, 6, 7, 8, 9, and 10 LPM and found to be 52.86%, 63.7%, 84.12%, 73.54%, 68.76%, and 61.76%, respectively.

Thus, from the present research work it can be concluded that the NePCM-nanofluid may be considered as the viable solution for the performance enhancement of PVT systems. It can also be noted that the mass flow rate of fluid and ambient conditions are very essential parameters for the efficient working of any developed PVT system.

Acknowledgement
This research was not funded by any grant.

References

[1] Ramachandra, T. V., Rishabh Jain, and Gautham Krishnadas. "Hotspots of solar potential in India." *Renewable and Sustainable Energy Reviews* 15, no. 6 (2011): 3178-3186. https://doi.org/10.1016/j.rser.2011.04.007
[2] Ministry of New and Renewable Energy. "Annual Report 2022-23." *Government of India*, 2023.
[3] Al-Shahri, Omar A., Firas B. Ismail, M. A. Hannan, MS Hossain Lipu, Ali Q. Al-Shetwi, R. A. Begum, Nizar FO Al-Muhsen, and Ebrahim Soujeri. "Solar photovoltaic energy optimization methods, challenges and issues: A comprehensive review." *Journal of Cleaner Production* 284 (2021): 125465. https://doi.org/10.1016/j.jclepro.2020.125465
[4] Joshi, Sandeep S., and Ashwinkumar S. Dhoble. "Photovoltaic-Thermal systems (PVT): Technology review and future trends." *Renewable and Sustainable Energy Reviews* 92 (2018): 848-882. https://doi.org/10.1016/j.rser.2018.04.067
[5] Herng, Sam Yih, Mohd Afzanizam Mohd Rosli, Nurfahana Salimen, Safarudin Ghazali Herawan, and Faridah Hussain. "Performance Evaluation of Photovoltaic Thermal using MgO Nanofluid." *Journal of Advanced Research in Fluid Mechanics and Thermal Sciences* 109, no. 2 (2023): 184-209. https://doi.org/10.37934/arfmts.109.2.184209
[6] Sato, Daisuke, and Noboru Yamada. "Review of photovoltaic module cooling methods and performance evaluation of the radiative cooling method." *Renewable and Sustainable Energy Reviews* 104 (2019): 151-166. https://doi.org/10.1016/j.rser.2018.12.051
[7] Nazer, Mohamed, Muhammad Fadzrul Hafidz Rostam, Se Yong Eh Noum, Mohammad Taghi Hajibeigy, Kamyar Shameli, and Ali Tahaei. "Performance analysis of photovoltaic passive heat storage system with microencapsulated paraffin wax for thermoelectric generation." *Journal of Research in Nanoscience and Nanotechnology* 1, no. 1 (2021): 75-90. https://doi.org/10.37934/jrnn.1.1.7590
[8] Siecker, J., Kanzumba Kusakana, and B. P. Numbi. "A review of solar photovoltaic systems cooling technologies." *Renewable and Sustainable Energy Reviews* 79 (2017): 192-203. https://doi.org/10.1016/j.rser.2017.05.053
[9] Omisanya, M. I., A. K. Hamzat, S. A. Adedayo, I. A. Adediran, and T. B. Asafa. "Enhancing the thermal performance of solar collectors using nanofluids." In *IOP Conference Series: Materials Science and Engineering*, vol. 805, no. 1, p. 012015. IOP Publishing, 2020. https://doi.org/10.1088/1757-899X/805/1/012015
[10] Loon, Yew Wai, and Nor Azwadi Che Sidik. "A comprehensive review of recent progress of nanofluid in engineering application: Microchannel heat sink (MCHS)." *Journal of Advanced Research in Applied Sciences and Engineering Technology* 28, no. 2 (2022): 1-25. https://doi.org/10.37934/araset.28.2.125
[11] Minea, Alina Adriana. "Hybrid nanofluids based on Al2O3, TiO2 and SiO2: numerical evaluation of different approaches." *International Journal of Heat and Mass Transfer* 104 (2017): 852-860. https://doi.org/10.1016/j.ijheatmasstransfer.2016.09.012
[12] Rosli, Mohd Afzanizam Mohd, Siti Nur Dini Noordin Saleem, Nortazi Sanusi, Nurfarhana Salimen, Safarudin Gazali Herawan, and Qaharuddin Abdullah. "Performance Optimization of a Simulation Study on Phase Change Material for Photovoltaic Thermal." *CFD Letters* 14, no. 9 (2022): 32-51. https://doi.org/10.37934/cfdl.14.9.3251
[13] Al-Zurfi, Hazim A., Muna Ali Talib, Qasim H. Hassan, and Ghaith J. Aljabri. "A Numerical Study to Improve the Efficiency of Solar Collector used for water heating using Phase Change Material." *Journal of Advanced Research in Numerical Heat Transfer* 17, no. 1 (2024): 1-13. https://doi.org/10.37934/arnht.17.1.113
[14] Al Imam, M. F. I., R. A. Beg, M. S. Rahman, and M. Z. H. Khan. "Performance of PVT solar collector with compound parabolic concentrator and phase change materials." *Energy and Buildings* 113 (2016): 139-144. https://doi.org/10.1016/j.enbuild.2015.12.038
[15] Browne, Maria C., Brian Norton, and Sarah J. McCormack. "Heat retention of a photovoltaic/thermal collector with PCM." *Solar Energy* 133 (2016): 533-548. https://doi.org/10.1016/j.solener.2016.04.024
[16] Hasan, Ahmed, S. J. McCormack, M. J. Huang, and Brian Norton. "Evaluation of phase change materials for thermal regulation enhancement of building integrated photovoltaics." *Solar Energy* 84, no. 9 (2010): 1601-1612. https://doi.org/10.1016/j.solener.2010.06.010
[17] Kazanci, Ongun B., Martynas Skrupskelis, Pavel Sevela, Georgi K. Pavlov, and Bjarne W. Olesen. "Sustainable heating, cooling and ventilation of a plus-energy house via photovoltaic/thermal panels." *Energy and Buildings* 83 (2014): 122-129. https://doi.org/10.1016/j.enbuild.2013.12.064
[18] Hasan, Ahmad, Sarah Josephine McCormack, Ming Jun Huang, and Brian Norton. "Energy and cost saving of a photovoltaic-phase change materials (PV-PCM) system through temperature regulation and performance enhancement of photovoltaics." *Energies* 7, no. 3 (2014): 1318-1331. https://doi.org/10.3390/en7031318

[19] Fiorentini, Massimo, Paul Cooper, and Zhenjun Ma. "Development and optimization of an innovative HVAC system with integrated PVT and PCM thermal storage for a net-zero energy retrofitted house." *Energy and Buildings* 94 (2015): 21-32. https://doi.org/10.1016/j.enbuild.2015.02.018

[20] Karunamurthy, K., K. Murugumohankumar, and S. Suresh. "Use of CuO nano-material for the improvement of thermal conductivity and performance of low temperature energy storage system of solar pond." *Digest Journal of Nanomaterials and Biostructures* 7, no. 4 (2012): 1833-1841.

[21] Khanjari, Y., F. Pourfayaz, and A. B. Kasaeian. "Numerical investigation on using of nanofluid in a water-cooled photovoltaic thermal system." *Energy Conversion and Management* 122 (2016): 263-278. https://doi.org/10.1016/j.enconman.2016.05.083

[22] Rejeb, Oussama, Mohammad Sardarabadi, Christophe Ménézo, Mohammad Passandideh-Fard, Mohamed Houcine Dhaou, and Abdelmajid Jemni. "Numerical and model validation of uncovered nanofluid sheet and tube type photovoltaic thermal solar system." *Energy Conversion and Management* 110 (2016): 367-377. https://doi.org/10.1016/j.enconman.2015.11.063

[23] Minea, Alina Adriana. "Hybrid nanofluids based on Al_2O_3, TiO_2 and SiO_2: numerical evaluation of different approaches." *International Journal of Heat and Mass Transfer* 104 (2017): 852-860. https://doi.org/10.1016/j.ijheatmasstransfer.2016.09.012

[24] Sardarabadi, Mohammad, Mohammad Passandideh-Fard, Mohammad-Javad Maghrebi, and Mohsen Ghazikhani. "Experimental study of using both ZnO/water nanofluid and phase change material (PCM) in photovoltaic thermal systems." *Solar Energy Materials and Solar Cells* 161 (2017): 62-69. https://doi.org/10.1016/j.solmat.2016.11.032

[25] Hosseinzadeh, Mohammad, Mohammad Sardarabadi, and Mohammad Passandideh-Fard. "Energy and exergy analysis of nanofluid based photovoltaic thermal system integrated with phase change material." *Energy* 147 (2018): 636-647. https://doi.org/10.1016/j.energy.2018.01.073

[26] Hassan, Ali, Abdul Wahab, Muhammad Arslan Qasim, Muhammad Mansoor Janjua, Muhammad Aon Ali, Hafiz Muhammad Ali, Tufail Rehman Jadoon, Ejaz Ali, Ahsan Raza, and Noshairwan Javaid. "Thermal management and uniform temperature regulation of photovoltaic modules using hybrid phase change materials-nanofluids system." *Renewable Energy* 145 (2020): 282-293. https://doi.org/10.1016/j.renene.2019.05.130